ELSEVIER

Intermetallics 7 (1999) 5–9

Intermetallics

Phase stability and elastic moduli of Cr_2Nb by first-principles calculations

Suklyun Hong*, C.L. Fu

Metals and Ceramics Division, Oak Ridge National Laboratory, Oak Ridge, TN 37831-6114, USA

Received 11 November 1997; accepted 16 December 1997

Abstract

The phase stability and elastic moduli of Cr_2Nb are investigated by first-principles calculations. Heats of formation are calculated and compared for the three Laves phases (C15, C14, and C36). It is found that the C15 phase is the ground-state structure with the lowest energy and the C36 phase is an intermediate state between C15 and C14. These three phases, however, are very close in energy, indicating low stacking fault energies in this system. For the ground-state C15 phase, we calculate three elastic constants from which the shear and Young's moduli are obtained. It is found that these calculated moduli are smaller than the experimental values obtained from polycrystals. © 1998 Elsevier Science Ltd. All rights reserved.

Keywords: A. Cr_2Nb Laves phases; Phase stability; First-principles calculations; FLAPW; B. Elastic properties

1. Introduction

High-temperature structural materials [1] are critically needed for improving the thermal efficiency and reliability of energy conversion systems and advanced engine systems. Of the potential candidate systems, Laves phases are the most abundant yet least utilized intermetallic phases. Because of some unique properties, including high-melting temperatures, high-elevated temperature strengths, reasonable oxidation resistance, and excellent creep properties, Laves phases have an unusual potential for a wide variety of structural applications. Unfortunately, this potential has not been exploited, largely because of their tendency for low temperature brittleness, which is a common disadvantage of these materials. At present, only limited scientific efforts have been focused on understanding and improving their brittle fracture behavior.

Laves phases include the face-centered cubic (fcc) C15 ($MgCu_2$), hexagonal C14 ($MgZn_2$) and C36 ($MgNi_2$) structures [2]. Among the three Laves phases, the C15 structure is expected to show better deformability than the other two phases because more independent slip systems are allowed in its fcc-based structure [3]. Of many C15 materials, Cr_2Nb appears to be very promising as shown in the experimental studies [4,5].

Using first-principles calculations, a fundamental understanding of the electronic and mechanical properties of Laves phases is of paramount importance, because such an understanding is essential for deriving the scientific principles to improve their physical and mechanical properties and for broadening the potential structural applications of these intermetallics. As a first step to achieve this goal, we perform the total-energy calculations to investigate their structural and elastic properties. In Section 2, a brief description on the calculational method and Laves structures is given. Results and discussion are given in Section 3.

2. Calculation method and Laves structures

We performed total-energy calculations for the three Laves phase structures of Cr_2Nb using the full-potential linearized augmented plane-wave (FLAPW) method [6] within the local-density approximation (LDA). The FLAPW method solves the local-density-functional equations without any shape approximation to the potential or charge density. The methodology has been described previously [7]. The atomic positions are relaxed by calculating Hellmann–Feynman forces acting on the atoms.

In order to calculate heats of formation, we calculated the bulk properties of Nb and Cr. For bcc Nb, we

* Corresponding author. E-mail: hongs@ornl.gov

0966-9795/98/$—see front matter © 1998 Elsevier Science Ltd. All rights reserved
PII: S0966-9795(98)00005-3

obtained a lattice constant of 3.24 Å and a bulk modulus of 169 GPa, in good agreement with the experimental values of 3.30 Å and 170.2 GPa, respectively. For bcc Cr, a lattice constant of 2.79 Å was obtained which is in fair agreement with the experimental value of 2.88 Å.

The C15 structure of Cr_2Nb is a fcc-based structure containing six atoms (2 formula units) in the primitive unit cell. It belongs to the space group $Fd\bar{3}m$-number 227 and Pearson symbol $cF24$ [8]. The C14 and C36 structures are hexagonal structures containing 12 and 24 atoms in the primitive unit cell, respectively. Both C14 and C36 structures belong to the same space group $P6_3/mmc$-number 194, although they are different in structure type and in Pearson symbol: C14 ($MgZn_2$) is $hP12$ and C36 ($MgNi_2$) is $hP24$ [8]. The C15, C14, and C36 structures may be considered as having three different kinds of stacking sequences: basically, C15 is ABC stacking along the ⟨111⟩ direction, and C14 is AB stacking along the ⟨0001⟩ direction, and C36 is ABAC stacking along the ⟨0001⟩ direction, in the topologically close-packed structure [3].

3. Results and discussion

3.1. Bulk properties

The results for the total energy as a function of unit cell volume are presented in Fig. 1. From these results, the equilibrium lattice constants, bulk moduli, and heats of formation are obtained.

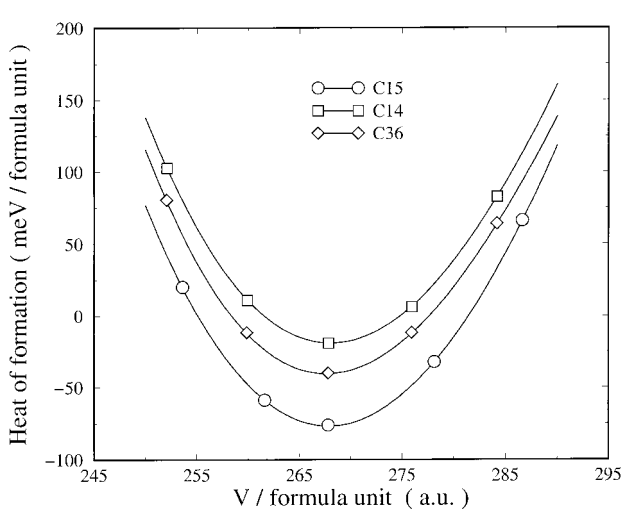

Fig. 1. The total energy as a function of unit formula volume for the C15 (circle), C14 (square) and C36 (diamond) structures of Cr_2Nb. The total energy for each phase is drawn as the heat of formation after subtraction of the sum of the total energies of the constituents: that is, the heat of formation is given by $E_{Cr_2Nb}-2E_{Cr}-E_{Nb}$ per formula unit. The symbols are connected by a smooth curve which is obtained by fitting the data by a third-order polynomial.

For the bulk fcc C15 (open circle in Fig. 1), we obtained a lattice constant of 6.822 Å and a bulk modulus of 252 GPa, in fairly good agreement with the experimental values of 6.991 Å [4] and 229.4 GPa [9], respectively. These results for structural properties are shown in Table 1 along with those of the C14 and C36 phases. Also, the results from an earlier study using the full-potential linear muffin-tin orbital (LMTO) method [3] are shown.

For the C14 phase, by using the experimental c/a ratio (being equal to 1.6336) [4], we first obtained a lattice constant of $a=4.823$ Å (thus $c=7.879$ Å), and a bulk modulus of 252 GPa. We then varied the c/a ratio at this theoretical volume to get the theoretical c/a ratio. Using this theoretical c/a ratio, the total energy was again calculated as a function of volume, which is shown as open squares in Fig. 1. We obtained the lattice constant of $a=4.829$ Å, $c/a=1.6288$ (thus $c=7.865$ Å) and a bulk modulus of 249 GPa. The lattice constants are to be compared with the experimental lattice constants of arc-cast alloys, which have a range of $a=4.97$ Å and $c=8.12$ Å for Nb-rich Cr_2Nb, and $a=4.94$ Å and $c=8.07$ Å for Cr-rich Cr_2Nb [4].

For the C36 phase, we varied the c/a ratio at the volume of four times theoretical volume of fcc C15 and obtained $c/a=3.2730$, and then varied the volume at this c/a ratio. From this calculation (open diamond in Fig. 1), we obtained the lattice constants of $a=4.819$ Å (thus $c=15.77$ Å) and a bulk modulus of 250 GPa. Note that for C14 and C36 the energy minimization has been achieved with respect to both the c/a ratio and unit cell volume.

Also, for both C14 and C36 phases, the atomic positions are optimized by calculating Hellmann–Feynman

Table 1
Structural properties and heats of formation of the three Laves phases of Cr_2Nb

		C15	C14	C36
Lattice constant	This work	6.82	4.83	4.82
a(Å)	LMTO[a]	6.83[b]	—	—
	Experiment[c]	6.991	4.94	—
Lattice constant	This work	—	7.87	15.77
c(Å)	Experiment[c]	—	8.07	—
c/a	This work	—	1.6288	3.2730
	Experiment[c]	—	1.6336	—
Bulk modulus	This work	252	249	250
B(GPa)	LMTO[a]	259	256	—
	Experiment[d]	229.4	—	—
Heat of formation	This work	−77	−19	−58
(meV)	LMTO[a]	−72.9	—	—

[a] Ref. [3].
[b] This lattice constant a is recalculated from the volume error −6.82% in Ref. [3].
[c] Ref. [4].
[d] Ref. [9].

forces acting on the atoms. For the C15 phase, the ideal atomic positions are not relaxed due to the symmetry constraint. The optimized atomic positions for the C14 and C36 phases are given in Tables 2 and 3. The coordinates are given in terms of lattice vectors: $\mathbf{r} = x_1\mathbf{a}_1 + x_2\mathbf{a}_2 + x_3\mathbf{a}_3$, where $\mathbf{a}_1 = (a/2)\hat{\mathbf{x}} - (\sqrt{3}a/2)\hat{\mathbf{y}}$, $\mathbf{a}_2 = (a/2)\hat{\mathbf{x}} + (\sqrt{3}a/2)\hat{\mathbf{y}}$, and $\mathbf{a}_3 = c\hat{\mathbf{z}}$.

It is shown in Fig. 1 that the equilibrium volume per formula unit is almost the same for each of C15, C14 and C36 structures: the lattice constant a of C15 is larger than those of C14 and C36 by almost a factor of $\sqrt{2}$, and the c/a ratio of C36 is almost twice that of C14. The theoretical volume change from C15 to C14 is about 0.06%, which is consistent with the measured volume change (0.03%) associated with the C14-to-C15 transformation for Cr_2Nb [10]. Also, the bulk moduli of three phases are almost identical, shown in Table 1.

For Cr_2Nb, the heat of formation is given by $E_{Cr_2Nb} - 2E_{Cr} - E_{Nb}$ per formula unit, where E_{Cr_2Nb}, E_{Cr}, and E_{Nb} are the total energy of Cr_2Nb, bulk Cr, and bulk Nb, respectively. The heats of formation of C15, C14, and C36 are found to be −77, −19, and −58 meV per formula unit, respectively. That is, the C15 phase is lower in energy than C14 by about 58 meV, and is also lower than C36 by about 19 meV per formula unit. We emphasize that these three phases are very close in energy. The calculated heats of formation are shown in Table 1 along with those using the LMTO method [3]. We see that C15 is a ground-state phase of Cr_2Nb and C36 is an intermediate phase with energy between those of C15 and C14 phases. Previously, Thoma and Perepezko [4] pointed out from X-ray diffraction measurements that the C36 phase may be an intermediate phase between the C15 and C14 phases although a complete analysis of the C36 phase was not given. Our theoretical calculations for structural stability supports their predictions.

Table 2
Optimized atomic positions in C14. Cr1 and Cr2 in this table are two different types of Cr atoms having different local symmetry. See text for details of coordinates x_i

Atom type	Coordinates		
	x_1	x_2	x_3
Cr1	0.0	0.0	0.0
	0.0	0.0	0.5
Cr2	0.3390	0.1695	1/4
	0.8305	0.1695	1/4
	0.8305	0.6610	1/4
	0.1695	0.8305	3/4
	0.1695	0.3390	3/4
	0.6610	0.8305	3/4
Nb	1/3	2/3	0.061
	1/3	2/3	0.439
	2/3	1/3	0.561
	2/3	1/3	0.939

Table 3
Optimized atomic positions in C36

Atom type	Coordinates		
	x_1	x_2	x_3
Cr1	1/3	2/3	0.1246
	1/3	2/3	0.3754
	2/3	1/3	0.6246
	2/3	1/3	0.8754
Cr2	1/2	0	0
	1/2	1/2	0
	0	1/2	0
	1/2	0	1/2
	0	1/2	1/2
	1/2	1/2	1/2
Cr3	0.16365	0.83635	1/4
	0.67270	0.83635	1/4
	0.16365	0.32730	1/4
	0.83635	0.67270	3/4
	0.83635	0.16365	3/4
	0.32730	0.16365	3/4
Nb1	0	0	0.0942
	0	0	0.4058
	0	0	0.5942
	0	0	0.9058
Nb2	2/3	1/3	0.1561
	2/3	1/3	0.3439
	1/3	2/3	0.6561
	1/3	2/3	0.8439

3.2. Elastic properties

For the C15 structure of Cr_2Nb, we evaluated the elastic constants. The new orthogonal lattice axes a_i' are related to the original ones a_j by $a_i' = (1+\varepsilon_{ij})a_j$, where $i,j = x, y, z$ and

$$\varepsilon_{ij} = \begin{pmatrix} e_1 & e_6/2 & e_5/2 \\ e_6/2 & e_2 & e_4/2 \\ e_5/2 & e_4/2 & e_3 \end{pmatrix} \tag{1}$$

is the strain tensor, and e_i's are the strain components. The elastic strain energy density is given by

$$U = \frac{1}{2}\sum_{i=1}^{6}\sum_{j=1}^{6}\tilde{C}_{ij}e_ie_j \tag{2}$$

where $C_{ij} = \frac{1}{2}(\tilde{C}_{ij} + \tilde{C}_{ji})$ and C_{ij}'s are the elastic constants [11]. The cubic structure has only three independent elastic constants C_{11}, C_{12}, and C_{44}. To determine three elastic constants, we need three relations, which can be obtained, for example, by considering the following three strain tensors: (i) $e_1 = e_2 \equiv e$ and $e_3 = -2e$, that is, tetragonal distortion at fixed volume, (ii) $e_1 = e_2 \equiv e$, and (iii) $e_6 = e$, where the unspecified strain components are

Table 4
Three calculated elastic constants (in units of GPa) at both theoretical and experimental volumes for C15 Cr_2Nb

	C_{11}	C_{12}	C_{44}
Theoretical volume	316	216	71
Experimental volume	250	170	58

zero for each of these cases. Therefore, three relations (i) $U=3(C_{11}-C_{12})e^2$, (ii) $U=(C_{11}+C_{12})e^2$, and (iii) $U=\frac{1}{2}C_{44}e^2$ are obtained. We calculated the total energies according to the above three kinds of lattice distortions and fitted the calculated values to third-order polynomials to get the elastic constants. We obtained $C_{11}=316$ GPa, $C_{12}=216$ GPa, and $C_{44}=71$ GPa at the theoretical lattice constant, which are shown in Table 4. To our knowledge, there have been no experimental measurements on the single crystal elastic constants of C15 Cr_2Nb so far. We should therefore consider the elastic moduli such as bulk, shear and Young's moduli, for comparison with experimental results.

From the results of the elastic constants, we obtained the elastic anisotropy ratio A,

$$A = \frac{2C_{44}}{C_{11} - C_{12}} \tag{3}$$

bulk modulus B, Young's modulus E, shear modulus G, and Poisson's ratio ν. In the Voigt average [12], the Young's and shear moduli in the cubic systems are given by

$$E_V = \frac{(C_{11} - C_{12} + 3C_{44})(C_{11} + 2C_{12})}{2C_{11} + 3C_{12} + C_{44}} \tag{4}$$

$$G_V = \frac{1}{5}(C_{11} - C_{12} + 3C_{44}) \tag{5}$$

while in the Reuss average [12] they are given by

$$E_R = 5/(3S_{11} + 2S_{12} + S_{44}) \tag{6}$$

$$G_R = 5/(4S_{11} - 4S_{12} + 3S_{44}) \tag{7}$$

with the relations $C_{44}=1/S_{44}$, $C_{11}-C_{12}=(S_{11}-S_{12})^{-1}$, and $C_{11}+2C_{12}=(S_{11}+2S_{12})^{-1}$ in the cubic systems. Knowing E and G, the bulk modulus B and the Poisson's ratio ν can be calculated from the isotropic relations

$$\nu = \frac{E}{2G} - 1 \tag{8}$$

$$B = \frac{EG}{3(3G - E)} = \frac{1}{3}(C_{11} + 2C_{12}) \tag{9}$$

Note that the bulk modulus is the same in both Voigt and Reuss averages in cubic systems. These results are shown in Table 5 along with the experimental values measured from the resonant ultrasound spectroscopy for polycrystals [9]. Note that the bulk modulus obtained from the relation (9) is very close to that of 252 GPa calculated directly from energy vs volume curve shown in Fig. 1.

While the calculated bulk modulus is larger by 9–10% than the experimental values, the calculated shear and Young's moduli are smaller than the experimental values by about 23 and 21%, respectively. Usually, the calculated elastic moduli are larger than the experimental values. It is because the calculation is for the ground-state properties and the calculated LDA lattice constants are always smaller than the experimental ones by about 2%. For the present case, however, the calculated shear and Young's moduli are smaller than the measured values obtained from polycrystals. The reason for this is unclear at this point.

So far we have mentioned the elastic properties at the theoretical volume. In fact, we have also examined the elastic constants at the experimental lattice constant. The calculational procedures are identical to those used for the theoretical lattice constant. The total energies as a function of lattice strains are then fitted to third-order polynomials. From the coefficients of the quadratic terms, we obtained the elastic constants: $C_{11}=250$ GPa, $C_{12}=170$ GPa, and $C_{44}=58$ GPa, which are also shown in Table 4. These elastic constants give smaller elastic moduli than those at the theoretical lattice constant (Table 5). As a result, the calculated bulk modulus,

Table 5
Elastic moduli derived from three elastic constants at both theoretical and experimental volumes are compared with the experimental values

		A	B(GPa)	E(GPa)	G(GPa)	ν
Theoretical volume	Theory (Voigt average)	1.41	249 (252)	173	62	0.384
	Theory (Reuss average)	—	249 (252)	168	61	0.387
Experimental volume	Theory (Voigt average)	1.45	197	140	51	0.381
	Theory (Reuss average)	—	197	136	49	0.385
	Experiment (Ref. 9)	—	229.4	214.1	79.6	0.34

A, B, E, G, and ν represent elastic anisotropy ratio, bulk modulus, Young's modulus, shear modulus and Poisson's ratio, respectively. The bulk modulus in the parenthesis was calculated directly from the energy versus volume curve shown in Fig. 1.

shear and Young's moduli at the experimental volume are smaller than the measured elastic moduli by about 14, 38 and 36%, respectively.

4. Conclusion

We performed the total-energy calculations to investigate the phase stability of Cr_2Nb. The calculation includes lattice constants, bulk moduli, and heats of formation. The results are in good agreement with available experiments. From these, it is found that C15 is a ground-state structure of Cr_2Nb, and C36 is an intermediate state between C15 and C14. They are very close in energy, so the stacking fault energies should be very small. The results on the stacking fault energy will be published elsewhere. For the C15 Cr_2Nb, we calculated the elastic constants. The calculated shear and Young's moduli are smaller than the experimental values.

Acknowledgements

The authors would like to thank Xindong Wang and M. H. Yoo for many helpful discussions. The research was sponsored by the Division of Materials Sciences, Office of Basic Energy Sciences, US Department of Energy under contract DE-AC05-96OR22464 with Lockheed Martin Energy Research Corporation.

References

[1] Pope DP, Liu CT. In: Tien JK, Caulfield T, editors. Superalloys, Supercomposites and Superceramics. New York, Academic Press, 1989:583.
[2] Westbrook JH. (ed.), Intermetallic Compounds. New York, John Wiley & Sons, 1967.
[3] Ormeci A, Chu F, Wills JM, Mitchell TE, Albers RC, Thoma DJ, Chen SP. Phys Rev 1996;B54:12753.
[4] Thoma DJ, Perepezko JH, Mater Sci Eng 1992;A156:97.
[5] Takeyama M, Liu CT. Mater Sci Eng 1991;A132:61.
[6] Wimmer E, Krakauer H, Weinert M, Freeman AJ. Phys Rev 1981;B24:864.
[7] Fu CL. J Mater Res, 1990;5:971; Fu CL, Yoo MH. Phil Mag Lett 1990;62:159.
[8] Daams LC, Villars P, van Vucht JHN. Atlas of crystal structure types for intermetallic phases. ASM International, Materials Park, OH, 1991.
[9] Chu F, Thoma DJ, He Y, Mitchell TE, Chen SP, Perepezko JH. In: High temperature structural intermetallic alloys VI, MRS Symposium Proceedings, 1995;364:1089. Chu F, He Y, Thoma DJ, Mitchell TE. Scripta Met et Mater 1995;33:1295.
[10] Kumar KS, Liu CT. Acta Metall 1997;45:3671.
[11] Kittel C. Introduction to solid state physics, 4th edn. New York, John Wiley & Sons, 1971, pp. 133–156.
[12] Hearmon RFS. An introduction to applied anisotropic elasticity. London, Oxford University Press, 1961:41–44.